

Lifetime of quasi-particles in the nearly-free electron metal Sodium

D.V. Potorochin,^{1,2,3,4} R. Kurlito,^{5,6} O.J. Clark,⁷ E.D.L. Rienks,⁷ J. Sánchez-Barriga,⁷
F. Roth,^{2,8} V. Voroshnin,⁷ A. Fedorov,⁵ W. Eberhardt,⁹ B. Büchner,^{5,10} and J. Fink^{5,10,*}

¹European XFEL, Holzkoppel 4, 22869 Schenefeld, Germany

²Institute of Experimental Physics, TU Bergakademie Freiberg, Leipziger Straße 23, 09599 Freiberg, Germany

³ITMO University, Kronverksky prospekt 49, 197101 Saint Petersburg, Russian Federation

⁴Deutsches Elektronen-Synchrotron DESY, Notkestrasse 85, D-22607 Hamburg, Germany

⁵Leibniz Institute for Solid State and Materials Research Dresden, Helmholtzstr. 20, D-01069 Dresden, Germany

⁶Department of Physics, University of Colorado, Boulder, CO, 80309, USA

⁷Helmholtz-Zentrum Berlin, Albert-Einstein-Strasse 15, 12489 Berlin, Germany

⁸Center for Efficient High Temperature Processes and Materials Conversion (ZeHS), 09599 Freiberg, Germany

⁹Center for Free-Electron Laser Science/DESY, 22607 Hamburg, Germany

¹⁰Institut für Festkörperphysik, Technische Universität Dresden, D-01062 Dresden, Germany

(Dated: December 2, 2021)

We report a high-resolution angle-resolved photoemission (ARPES) study of the prototypical nearly-free electron metal Sodium. The observed mass enhancement is in qualitative agreement with previous studies [PRL **55**, 1912 (1985)]. The new results on the lifetime broadening demand theories which go beyond the random phase approximation. On the other hand, our results do not support the discussed strong coupling of the conduction electrons to spin fluctuations. Moreover, a comparison with earlier electron energy-loss data on Sodium [PRB **40**, 10181 (1989)] yields a strong reduction of the mass enhancement of dipolar electron-hole excitations compared to that of monopole hole excitations, measured by ARPES. Finally, our results on the lifetime of hot electrons in Na, 70 eV above the Fermi level differ strongly from existing theoretical calculations and experiments on the mean-free path of hot electrons in simple metals.

Introduction. The understanding of electron-electron ($e - e$) many-body interactions in metals is an ongoing challenge in solid-state physics since many decades. This interaction is of great interest because it determines transport, thermal, and magnetic properties of metals. There are also many indications, that $e - e$ interaction, e.g. spin fluctuations [1] mediates unconventional superconductivity in cuprates and ferropnictides. These correlated materials are the subject of numerous experimental and theoretical studies during the last decades. Very often, they start from the classical behavior of normal metals (Fermi liquids) assuming that these are well understood.

Here we report a study of the simplest nearly-free electron metal Na. Even in this prototypical Fermi liquid metal, there are unresolved issues. Numerous attempts have been made to explain the mass enhancement $m^*/m = 1.28$, derived from the bandwidth reduction of the occupied states, observed in angle-resolved photoemission spectroscopy (ARPES) [2, 3] experiments from the Plummer group [4–6]. The mass renormalization is related to the real part of the self-energy $\Re\Sigma$. Various state-of-the-art many-body techniques were used, starting with the random phase approximation (RPA) [7], the GW formalism with all types of approximations (GW+) [8–12]. Correlation effects have been discussed in Refs. [13–15]. There are ongoing discussions about the influence of spin fluctuations [16]. More recently, a strong increase of the scattering rate Γ due to a strong coupling to spin fluctuations was predicted, but not a corresponding increase of the mass enhancement [17]. Γ is related

to the inverse lifetime τ and to the imaginary part of the self-energy by the relation $\Gamma = -2Z\Im\Sigma$, where Z is the renormalization function, which for a less correlated material is expected to be constant and close to the Fermi level equal to $Z=m/m^*$ [18].

The early ARPES studies on the mass enhancement of the quasi-particles in Na [4–6] were performed with an energy resolution of 0.3 eV. No linewidth analysis has been performed in these studies. Here we report not only on the mass enhancement, but also on the energy dependence of the lifetime broadening with an energy resolution, which is improved by a factor of 10 compared to the earlier experiments. To the best of our knowledge, no data on the lifetime of excited holes in Na have been published in the literature.

The central result of our ARPES study is that our data do not support a strong enhancement of the scattering rate due to a coupling to spin fluctuations. This is at variance with the theoretical work of Ref. [17]. Furthermore, a comparison with earlier electron energy-loss spectroscopy (EELS) data on Na [19] yields a strong reduction of the mass enhancement of dipolar electron-hole excitations compared to that of monopole hole excitations, measured by ARPES. Moreover, the final state lifetime broadening at a photon energy of 70 eV is strongly reduced when compared with various theoretical calculations.

Based on our new ARPES data we hope that we contribute to the general understanding of many-body problems in normal metals (Fermi liquids), which may also help to understand the normal state of cuprate supercon-

ductors (marginal Fermi liquids [20]), and iron pnictides which show “super Planckian scattering rates” [21–23].

Experimental. The experiments were performed at the 1² ARPES endstation using the UE 112-PGM-2a beamline. Additional experiments were performed at the RGLB-2 end station at the U125-2-PGM beamline. As a substrate we used a W(110) single crystal. This crystal was cleaned before deposition by annealing in O atmosphere (1×10^{-7} mbar) at 1200 °C followed by flashing at 2200 °C. The quality of the W (110) surface was verified by LEED experiments, core level spectroscopy on the W 4*f* level, and by ARPES experiments.

Na was evaporated out of a Mo crucible on the single crystalline W substrate, cooled to 20 K. Subsequently, the sample was annealed for 15 minutes at room temperature. Most of the results reported here were obtained from a Na (110) film having a thickness of about 15 nm. During measurements, the temperature of the crystal was 20 K. The base pressure of the experimental setup was better than $6 \cdot 10^{-11}$ mbar. Photoelectrons were detected with a Scienta R8000 electron analyzer. The overall experimental energy and momentum resolutions were set to 30 meV and 0.2° , respectively.

Experimental results. In Fig. 1 we show an energy-momentum distribution map measured with a photon energy of $h\nu = 70$ eV along $k_{\parallel} = k_y = \Gamma - N = \langle 100 \rangle$ at a k_z value corresponding to the Γ point in the fifth Brillouin zone (BZ). The Γ point has been determined from similar spectra measured for various photon energies. We have determined the dispersion $E(k)$ by fitting momentum distribution curves (MDC) with Lorentzians. The white dashed line is a fit of the derived dispersion with a parabola.

The spectral weight at the bottom of the band is rather low when compared with that at the Fermi level. The reason for this is related to matrix element effects. The initial state has predominantly *s* character, i.e., it is even with respect to the $k_x - k_z$ mirror plane. We measured with photons having a horizontal polarization. This means the dipole operator is even relative to that mirror plane. The vanishing intensity could indicate that the final states, which according to dipole excitation must be of *p*-character, are predominantly odd with respect to the scattering plane. The situation is very similar to our previous study of the waterfall dispersion of the spectral weight in Nd_2CuO_4 [24].

In Fig. 2 we depict the Fermi surface of Na (110) measured with a photon energy of $h\nu = 70$ eV in the $k_z = \Gamma, k_x - k_y$ plane. The data were derived by a summation of intensities in an energy range of 0.015 eV close to the Fermi level. The Fermi surface is close to a circle as expected for a nearly-free electron metal. The Fermi wave vector along the k_y line is $k_F = 0.91$ 1/Å. The deviations from a circular Fermi surface detected in the present experiment are caused possibly by a flattening and splitting of the dispersion due to the proximity to

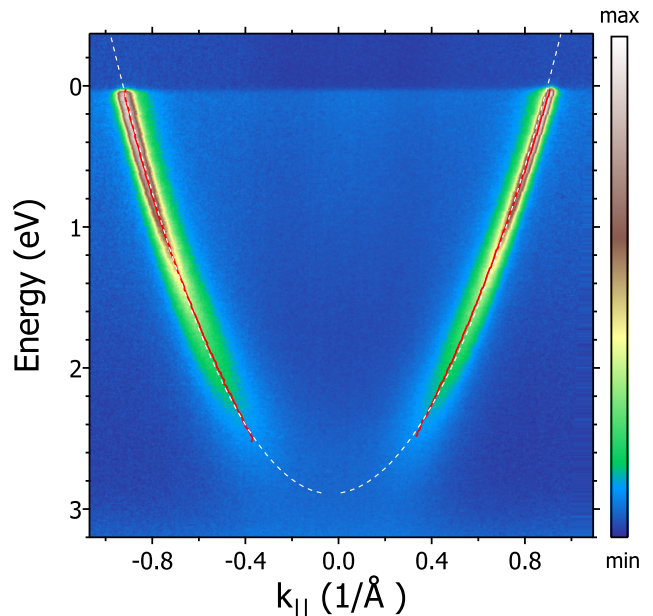


FIG. 1. Experimental energy-momentum distribution map of Na measured along the k_y direction using horizontally polarized photons with an energy of $h\nu = 70$ eV. Red line: dispersion derived from a Lorentzian fit to momentum distribution curves. White dashed line: fit of the maxima of the Lorentzians with a parabolic dispersion.

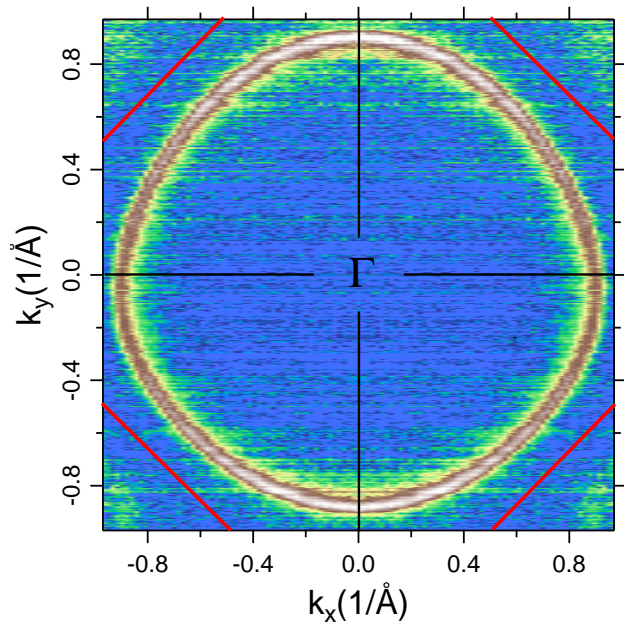


FIG. 2. Experimental Fermi surface map of Na (110) measured with horizontally ($\parallel k_x$) polarized photons with an energy of $h\nu = 70$ eV. The data are symmetrized relative to $k_x = 0$. Red lines: part of the Brillouin zone.

the Brillouin zone (BZ).

In the corners of Fig. 2 we detect a faint signal of the Fermi surface of the second BZ. This observation indi-

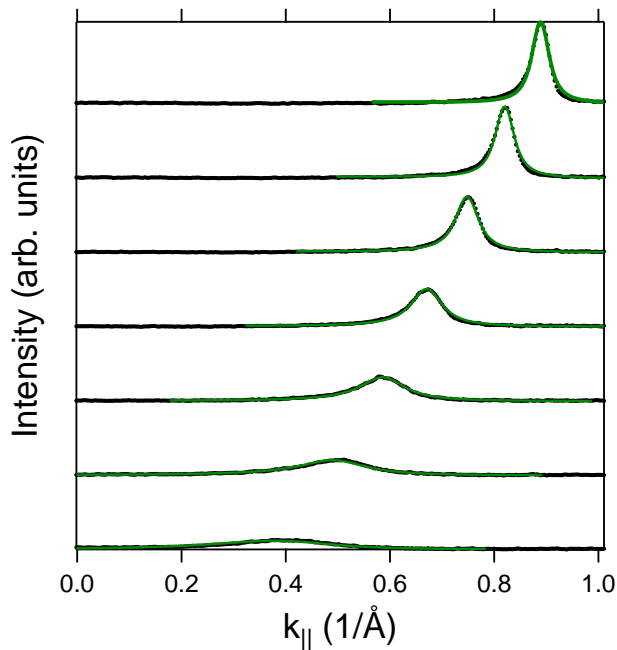


FIG. 3. Waterfall plot of ARPES momentum distribution curves of the valence band as a function of energy (black dots) in the energy range $0.103 \leq E \leq 2.263$ eV, measured along k_y (see Fig. 1 and 2). Green line: “all-at-once” fits of the spectral function with energy dependent lifetime broadening and including corrections from finite energy and momentum resolution.

cates that the orientation of the Na (110) single crystal is along the main high symmetry lines. This also supports that the momentum distribution map, presented in Fig. 1, is measured along the $\langle 100 \rangle$ (k_y) direction.

In Fig. 3 we present a waterfall plot of momentum distribution curves as a function of energy together with an “all at once fit” [25]. For the fit we use a quartic dispersion $E(k) = W - \gamma_1 k^2 - \gamma_2 k^4$. A small deviation from a free-electron parabolic dispersion was also derived from band structure calculations for Na [26]. From the fit we obtain the following parameters: $W = 2.78$ eV, $\gamma_1 = 3.77$ eV \AA^2 , $\gamma_2 = -0.49$ eV \AA^4 , and the total line width broadening $\Gamma(E)_{\text{exp}}$, corrected for finite experimental resolution, for each energy.

We emphasize, that we do not use the traditional method for the evaluation of the energy dependence of the line width, i.e., fitting the momentum distribution curves with Lorentzians and multiplication the derived widths in momentum space with the velocity. Rather we fit the two-dimensional data with the spectral function described with parameters related to the width in energy space at each energy.

To obtain the line width broadening $\Gamma(E)$ due to $e-e$ interaction, we have to subtract contributions from elastic scattering Γ_{el} and/or a broadening due to a finite inverse lifetime Γ_f of the final state. First, we assume

that the finite value $\Gamma_{\text{el}}(0)$ is completely determined by impurity scatterers. The constant mean distance d between the impurities is equal to $1/\Delta k$, where Δk is the momentum width at the Fermi level. Then the broadening due to elastic scattering is given by $v(E)\Delta k$, where $v(E)$ is the energy-dependent group velocity, taken from the experiment.

Second, we assume that the broadening at k_F is caused by final state effects. For normal emission, the final state broadening leads at the Fermi level to a broadening $(v_i/v_f)\Gamma_f$ [27]. This is proportional to v_i , as well. The case for off-normal detection is discussed in the Supplementary Material [28]. Then we come to the conclusion, that independent from the ratio between broadening due to elastic scattering and that from final state effects, a reasonable correction is proportional to $v_i = (W - E)^{0.5}$. Using this correction we obtain the inverse hole lifetime $\Gamma(E)$ which is depicted in Fig. 4.

The result can be fitted using the relation $\Gamma(E) = \Gamma_0 + \alpha E^n$ with $\alpha = 0.12$ and $n = 2.06$ (see Fig. 4). In the Supplementary Material [29] we depict the uncorrected curve which, at the Fermi level has a finite value of 0.12 eV. We also show that different ratios between broadening by elastic scattering and final state broadening almost do not change the values of α and n .

The real and the imaginary part of the self-energy are connected by the Kramers-Kronig transformation (KKT). This means that an enhancement of the scattering rate leads in tandem to an enhancement of the effective mass. Using the renormalization constant $Z = 0.6$ [17] we have calculated $\Im\Sigma(E) = \Gamma(E)/2Z$. Upon performing the KKT of $\Im\Sigma(E)$ we obtain $\Re\Sigma(E)$. From this the mass renormalization $m^*/m = 1 + \Re\Sigma(E)/E = 1.1$ can be calculated. This value is close to the value obtained directly from the band renormalization.

Discussion. The dispersion, derived from the data in Fig. 1 is very close to a parabola. This is expected for a nearly-free electron metal. A possible kink due to electron-phonon coupling would appear at very low energies because of the low Debye energy $\Theta_D = 0.013$ eV of Na [30] and it would be very weak because the electron-phonon coupling should be small in a nearly-free electron system such as the non-superconducting Na. In Table I we compare the band width and the mass enhancement (assuming a parabolic dispersion) with results from the Plummer group and theoretical calculations. The reduction of the band width when compared with that from LDA calculations [26] $W_{\text{LDA}} = 3.18$ eV is slightly less than that of the early ARPES study. Correspondingly, also the mass enhancement is slightly smaller. On the other hand, the deviations compared to the earlier values are not so pronounced. This means that the discussion of the band width reduction should follow earlier work. The free electron RPA calculations yield mass enhancements which are too small and the GW approximation or local field corrections are needed to describe the experimental

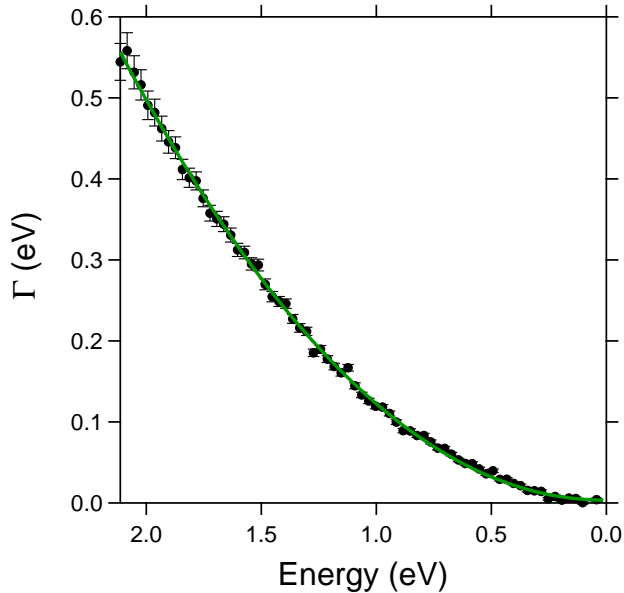


FIG. 4. Inelastic scattering rates Γ of electrons in Na as a function of energy. Black dots: corrected ARPES data derived from the fit presented in Fig. 3. Green solid line: fit with $\Gamma = \alpha E^n$ with $\alpha = 0.12$ and $n = 2.06$.

data (see Table I).

The energy dependence of the line width is almost perfectly quadratic. The exponent n is very close to two. The quadratic energy dependence extends over a large energy range up to 2.2 eV corresponding to a temperature of 25000 K.

The prefactor α is considerably higher than that of the RPA free-electron value of Quinn and Ferrel ($\alpha = 0.076$) [7]. Because the real part of the self-energy, determining the band width, and the imaginary part, determining the lifetime, is connected via the KKT, this difference is expected when regarding the data in Table I. Thus, also our data on the lifetime broadening demand that one has to go *beyond* RPA. Theoretical calculations using the GW approximation or local field corrections are closer to the experimental data. On the other hand, the calculations by Lischner *et al.* [17] postulating the importance of spin fluctuations for the scattering rate yield a much too high pre-factor α (see Table I). Thus our experimental results do not support the proposed strong coupling of the conduction electrons to spin fluctuations in Na.

Comparing the α value of the valence electrons in Na with $\alpha = 0.24$ derived for surface states in the 3d metal Mo [31] signals the expected enhanced scattering rate in 4d metals relative to that of *sp* metals.

Next we discuss a comparison of our ARPES data with data of interband and intraband excitations in Na [19] measured by EELS. From the cutoff of interband transitions a mass enhancement $m^*/m = 1.05 \pm 0.04$ was derived. A similar value $m^*/m=1.0$ was obtained from

TABLE I. ARPES data of Na compared with theoretical data from the literature: ARPES, present work; ARPES/KKT effective mass derived by a Kramers-Kronig transformation of the scattering rate; ARPES from Plummer's group; RPA FEG, free electron gas; RPA LDA; GW LDA + plus approximations; GW LDA SF plus spin fluctuations. W : band width, m^*/m mass renormalization using $W_{\text{LDA}} = 3.18$ eV from LDA calculations [26]. α : pre-factor from the fit of the corrected scattering rates. Γ_f : final state width.

	W (eV)	m^*/m	α (1/(eV))	Γ_f (eV)
ARPES ^a	2.78	1.11	0.12	0.6
ARPES/KKT ^b		1.1		
ARPES ^c	2.5-2.61	1.28		
RPA FEG ^d	2.96	1.10	0.05-0.077	3.3
RPA LDA ^e			0.1	3.3
GW + ^f	2.52-2.89	1.11-1.26	0.10-0.34	
GW LDA SF ^g	2.51	1.27	0.47	

^a ARPES, present work

^b ARPES+KKT, present work

^c Refs. [4-6]

^d Refs. [7, 9, 18, 32, 33]

^e Ref. [9]

^f Refs. [10, 17]

^g Ref. [17]

the analysis of zone boundary collective states (ZBCS), a combination of intraband and interband excitations from the band bottom to states near the BZ. The conflict between the ARPES and the EELS data can be explained in the following way: EELS measures inter- or intraband excitations, i.e., two particle or electron-hole excitations with dipole character. They are less screened than single-hole or monopole excitations detected in ARPES experiments.

Final state effects may have far-reaching implications for the interpretation of all ARPES data. E. g., in Ref. [34] it is claimed, that the mass renormalization of the valence electrons detected in ARPES is related to final state effects. This interpretation can be ruled out because a similar mass enhancement $m^*/m = 1.256$ has been detected in de-Haas-van-Alphen effect measurements [35].

From the momentum width at the Fermi level $\Delta k_F = 0.0185$ 1/Å it is possible to derive the mean free path of the photoelectrons with a photon energy of 70 eV in Na. Assuming that the broadening at E_F is predominantly caused by elastic scattering we obtain $\lambda(E=70 \text{ eV}) = 1/\Delta k_F \geq 54$ Å. This value is much larger than the value derived from core level photoelectron experiments $\lambda(E=70 \text{ eV}) = 8$ Å [36]. Furthermore, for normal emission, one can calculate the lifetime broadening of the final state $\Gamma_f = v_f \Delta k_F$. Using the free electron value for $v_f = 33.5$ eVÅ one obtains $\Gamma_f = 0.6$ eV. This value is much smaller than the one calculated on the basis of a coupling to plasmons in a free electron model (RPA) [18] or using RPA LDA [9] predicting $\Gamma_f = 3.3$ eV. This means that

our results on the final state broadening of hot electrons also require new theoretical investigations.

D.V.P. acknowledges support from the Russian Foundation for Basic Research (Grant no. 20-02-00489). J.S.-B. acknowledges financial support from the Impuls- und Vernetzungsfonds der Helmholtz-Gemeinschaft under grant No. HRSF-0067 (Helmholtz-Russia Joint Research Group).

* Corresponding author. E-mail address: J.Fink@ifw-dresden.de.

- [1] T. Dahm, V. Hinkov, S. V. Borisenko, A. A. Kordyuk, V. B. Zabolotnyy, J. Fink, B. Büchner, D. J. Scalapino, W. Hanke, and B. Keimer, *Nature Physics* **5**, 217 (2009).
- [2] A. Damascelli, Z. Hussain, and Z.-X. Shen, *Rev. Mod. Phys.* **75**, 473 (2003).
- [3] J. A. Sobota, Y. He, and Z.-X. Shen, *Rev. Mod. Phys.* **93**, 025006 (2021).
- [4] E. Jensen and E. W. Plummer, *PRL* **55**, 1912 (1985).
- [5] E. W. Plummer, *Physica Scripta* **T17**, 186 (1987).
- [6] I.-W. Lyo and E. W. Plummer, *Phys. Rev. Lett.* **60**, 1558 (1988).
- [7] J. J. Quinn and R. A. Ferrell, *PR* **112**, 812 (1958).
- [8] J. E. Northrup, M. S. Hybertsen, and S. G. Louie, *PRB* **39**, 8198 (1989).
- [9] J. S. Dolado, V. M. Silkin, M. A. Cazalilla, A. Rubio, and P. M. Echenique, *PRB* **64**, 195128 (2001).
- [10] M. Cazzaniga, *PRB* **86**, 035120 (2012).
- [11] J. S. Zhou, M. Gatti, J. J. Kas, J. J. Rehr, and L. Reining, *PRB* **97**, 035137 (2018).
- [12] S. Mandal, K. Haule, K. M. Rabe, and D. Vanderbilt, *Electronic correlation in nearly free electron metals with beyond-dft methods* (2021), arXiv:2101.03262 [cond-mat.str-el].
- [13] T. K. Ng and K. S. Singwi, *PRB* **34**, 7738 (1986).
- [14] F. Nilsson, L. Boehnke, P. Werner, and F. Aryasetiawan, *PRMATERIALS* **1**, 043803 (2017).
- [15] L. Craco and S. Leoni, *PRB* **100**, 115156 (2019).
- [16] X. Zhu and A. W. Overhauser, *PRB* **33**, 925 (1986).
- [17] J. Lischner, T. Bazhironov, A. H. MacDonald, M. L. Cohen, and S. G. Louie, *PRB* **89**, 081108 (2014).
- [18] B. I. Lundqvist, *phys. stat. sol. (b)* **32**, 273 (1969).
- [19] A. vom Felde, J. Sprösser-Prou, and J. Fink, *PRB* **40**, 10181 (1989).
- [20] C. M. Varma, P. B. Littlewood, S. Schmitt-Rink, E. Abrahams, and A. E. Ruckenstein, *PRL* **63**, 1996 (1989).
- [21] S. A. Hartnoll and A. P. Mackenzie, *Planckian dissipation in metals* (2021), arXiv:2107.07802 [cond-mat.str-el].
- [22] J. Fink, E. D. L. Rienks, M. Yao, R. Kurlito, J. Bannies, S. Aswartham, I. Morozov, S. Wurmehl, T. Wolf, F. Hardy, C. Meingast, H. S. Jeevan, J. Maiwald, P. Gegenwart, C. Felser, and B. Büchner, *PRB* **103**, 155119 (2021).
- [23] M. Hemmida, N. Winterhalter-Stocker, D. Ehlers, H.-A. K. von Nidda, M. Yao, J. Bannies, E. D. L. Rienks, R. Kurlito, C. Felser, B. Büchner, J. Fink, S. Gorol, T. Förster, S. Arsenijevic, V. Fritsch, and P. Gegenwart, *PRB* **103**, 195112 (2021).
- [24] E. D. L. Rienks, M. Lindroos, F. Roth, W. Tabis, G. Yu, M. Greven, and J. Fink, *Phys. Rev. Lett.* **113**, 137001 (2014).
- [25] R. Kurlito and J. Fink, *Journal of Electron Spectroscopy and Related Phenomena* **253**, 147127 (2021).
- [26] W. Y. Ching and J. Callaway, *PRB* **11**, 1324 (1975).
- [27] N. V. Smith, P. Thiry, and Y. Petroff, *Phys. Rev. B* **47**, 15476 (1993).
- [28] See Supplemental Material.
- [29] See Supplemental Material.
- [30] D. L. Martin, *PR* **124**, 438 (1961).
- [31] T. Valla, A. V. Fedorov, P. D. Johnson, and S. L. Hulbert, *Phys. Rev. Lett.* **83**, 2085 (1999).
- [32] L. Hedin, *PR* **139**, A796 (1965).
- [33] E. V. Chulkov, A. G. Borisov, J. P. Gauyacq, D. Sánchez-Portal, V. M. Silkin, V. P. Zhukov, and P. M. Echenique, *Chem. Rev.* **106**, 4160 (2006).
- [34] H. Yasuhara, S. Yoshinaga, and M. Higuchi, *PRL* **83**, 3250 (1999).
- [35] M. Elliott and W. R. Datars, *Journal of Physics F: Metal Physics* **12**, 465 (1982).
- [36] N. V. Smith, G. K. Wertheim, A. B. Andrews, and C.-T. Chen, *Surface Science* **282**, L359 (1993).

D.V. Potorochin,^{1,2,3,4} R. Kurlito,^{5,6} O.J. Clark,⁷ E.D.L. Rienks,⁷ J. Sánchez-Barriga,⁷
 F. Roth,^{2,8} V. Voroshnin,⁷ A. Fedorov,⁵ W. Eberhardt,⁹ B. Büchner,^{5,10} and J. Fink^{5,10,*}

¹European XFEL, Holzkoppel 4, 22869 Schenefeld, Germany

²Institute of Experimental Physics, TU Bergakademie Freiberg, Leipziger Straße 23, 09599 Freiberg, Germany

³ITMO University, Kronverksky prospekt 49, 197101 Saint Petersburg, Russian Federation

⁴Deutsches Elektronen-Synchrotron DESY, Notkestrasse 85, D-22607 Hamburg, Germany

⁵Leibniz Institute for Solid State and Materials Research Dresden, Helmholtzstr. 20, D-01069 Dresden, Germany

⁶Department of Physics, University of Colorado, Boulder, CO, 80309, USA

⁷Helmholtz-Zentrum Berlin, Albert-Einstein-Strasse 15, 12489 Berlin, Germany

⁸Center for Efficient High Temperature Processes and Materials Conversion (ZeHS), 09599 Freiberg, Germany

⁹Center for Free-Electron Laser Science/DESY, 22607 Hamburg, Germany

¹⁰Institut für Festkörperphysik, Technische Universität Dresden, D-01062 Dresden, Germany

(Dated: December 2, 2021)

In this supplement we present additional information on the corrections used for the evaluation of the lifetime of holes in the valence band of Na. In particular, we describe the corrections of the ARPES data from contributions of elastic scattering by impurities and by a broadening caused by the lifetime of the final state electrons.

The ARPES data on scattering rates determining the spectral function contain besides the inelastic scattering rates of the conduction electrons also contributions from elastic scattering due to impurities and contributions from the lifetime broadening of the excited photoelectron in the final state.

Usually, it is assumed that the elastic scattering rate Γ_{el} is independent of the energy E . It is caused by an elastic scattering from impurities which are separated by a mean distance d . The inverse lifetime $1/\tau_e = \Gamma_{el} = dv_i$, where v_i is the group velocity of the quasiparticles. Close to the Fermi level, it is a good approximation to assume a linear dispersion from which follows that v_i is constant and therefore Γ_{el} should be constant. On the other hand, in the present work we study the spectral weight over a large energy range and the dispersion is parabolic leading to an energy dependent velocity. Close to the Fermi level it is high while at the bottom of the band it is zero. Thus, the elastic scattering rate should be $\Gamma_{el}(E) = (v(E)_i/v_F)\Gamma_{el}(E_F)$.

In Fig. 1 we plot the total lifetime broadening derived from the ARPES data shown in Fig. 3 of the main paper. Different from the expected zero value at the Fermi level E_F , there is an offset, due to the elastic scattering and/or the final state broadening. Assuming that this offset is completely determined by a constant elastic scattering, which corresponds to the usual evaluation method, from a fit with $\Gamma = \Gamma_0 + \alpha E^n$, we obtain the parameters $n = 2.22$ and $\alpha = 0.089$. Subtracting the energy dependent elastic scattering being proportional to $(W - E)^{0.5}$, we derive the data depicted in Fig. 1 by green markers.

Part of the offset at the Fermi level can also be caused by final state effects. According to Ref.[1] the total experimental broadening Γ_{exp} is given by

$$\Gamma_{exp} = \frac{\frac{\Gamma_i}{|v_{i\perp}|} + \frac{\Gamma_f}{|v_{f\perp}|}}{\left| \frac{1}{v_{i\perp}} \left[1 - \frac{mv_{i\parallel} \sin^2 \Theta}{\hbar k_{\parallel}} \right] - \frac{1}{v_{f\perp}} \left[1 - \frac{mv_{f\parallel} \sin^2 \Theta}{\hbar k_{\parallel}} \right] \right|}. \quad (1)$$

Γ_i and Γ_f denote the lifetime width of the photohole (ini-

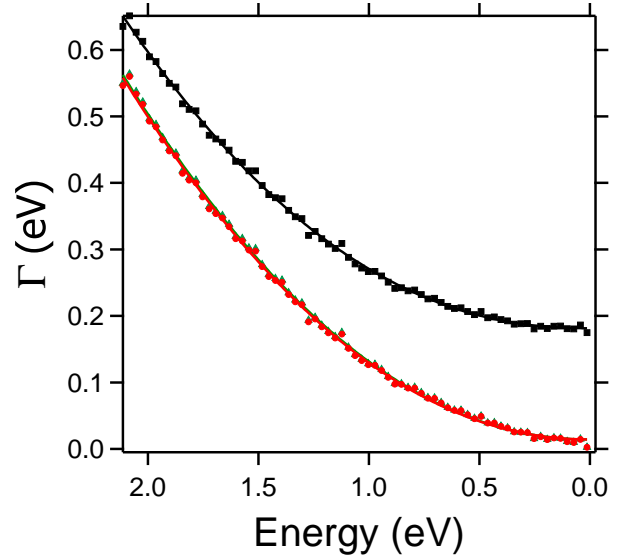


FIG. 1. Presentation of bare scattering rates derived from ARPES (black markers) together with data corrected for energy dependent elastic scattering (green markers) and data corrected for energy dependent final state broadening (red markers). The solid lines are least squares fit with $\Gamma = \Gamma_0 + \alpha E^n$.

tial state) and the photoelectron (final state), respectively. $v_{i\perp}$ and $v_{f\perp}$ are group velocities $\hbar v_{i\perp} = \frac{\partial E_i}{\partial k_{\perp}}$ and so forth. For these velocities we use a free-electron model. Θ is the angle between the electron-detection direction and the surface normal. Now we assume that the total broadening is completely caused by final state effects. Using Eq. (1), we derive data for the inelastic $e - e$ scattering rate of holes in the valence band Γ_i from the experimental ARPES data Γ_{exp} , corrected for final state broadening.

The data derived taken into account the final state broadening are shown in Fig. 1 by red markers. The

difference of the corrected data using the two methods is marginal. This is also obvious from the derived the fit parameters. For correction of elastic scattering we obtain $n = 2.06$ and $\alpha = 0.117$, while for the final state corrections the parameters are $n = 2.07$ and $\alpha = 0.115$.

This comparison shows, that the parameters describing the energy dependent $e - e$ scattering rates, presented in the main paper, are nearly independent of the origin of the offset.

* Corresponding author. E-mail address: J.Fink@ifw-dresden.de.

[1] N. V. Smith, P. Thiry, and Y. Petroff, Phys. Rev. B **47**, 15476 (1993).